



ELSEVIER

Contents lists available at SciVerse ScienceDirect

Biosensors and Bioelectronics

journal homepage: www.elsevier.com/locate/bios

Frozen assembly of gold nanoparticles for rapid analysis of antifreeze protein activity

Ji-In Park^{a,b}, Jun Hyuck Lee^{c,d}, Yunho Gwak^{a,b}, Hak Jun Kim^{c,d}, EonSeon Jin^{a,b,*}, Young-Pil Kim^{a,b,**}

^a Department of Life Science, Hanyang University, Seoul 133-791, Republic of Korea

^b Research Institute for Natural Sciences, Hanyang University, Seoul 133-791, Republic of Korea

^c Division of Polar Life Sciences, Korea Polar Research Institute, Incheon 406-840, Republic of Korea

^d Department of Polar Sciences, University of Science and Technology, Incheon 406-840, Republic of Korea

ARTICLE INFO

Article history:

Received 8 August 2012

Received in revised form

22 September 2012

Accepted 27 September 2012

Available online 4 October 2012

Keywords:

Gold nanoparticle

Frozen assembly

Antifreeze protein

Ice-binding protein

Thermal hysteresis

ABSTRACT

We report the novel activity-based detection of antifreeze protein (AFP), also known as ice-binding protein (IBP), using freeze-labile gold nanoparticles (AuNPs) in order to overcome labor-intensive and low throughput issues of the current method based on thermal hysteresis (TH). Upon the addition of either CnAFP from the Antarctic diatom *Chaetoceros neogracile* or LeIBP from the Arctic yeast *Leucosporidium* sp. to mercaptosuccinic acid-capped AuNP, the self-assembly of AuNPs was highly inhibited after a freezing/thawing cycle, leading to no color change in the AuNP solution. As a result, the aggregation parameter (E_{520}/E_{650}) of AuNP presented the rapid detection of both the concentration-dependent activity and stability of two AFPs with high sensitivity, where the detection range was 100-fold lower than that of the TH-based method. We suggest that our newly developed method is very suitable for simple and high-throughput measurement of AFP activity.

© 2012 Elsevier B.V. All rights reserved.

1. Introduction

Antifreeze proteins (AFPs), also known as ice-binding proteins (IBPs), are attractive research targets due to their ability to lower freezing temperatures through the inhibition of ice growth, allowing for the survival of many organisms that inhabit ice-laden environments (Chou, 1992; Garnham et al., 2011; Jorov et al., 2004). AFPs have evolved a non-colligative freezing mechanism, which essentially means that they are effective antifreeze agents at concentrations of 1/300th to 1/500th of those of other cryoprotectants, such as glycerol and sorbitol (Fletcher et al., 2001). Researchers are currently investigating ways to harness the cryoprotective properties of AFPs through their inclusion as food (Boonsupthip and Lee, 2003), cell (Carpenter and Hansen, 1992), or plant (Griffith and Yaish, 2004) preservatives. However, in spite of their potential applications to industry and cryomedicine, the current method for measuring antifreeze activity relies exclusively on thermal hysteresis (TH), which is the difference between melting and freezing points. This method has

a major drawback in that it needs to be performed by long-term observations of the ice-binding crystals over a temperature gradient using a nanoliter osmometer (Barrett, 2001; Kristiansen and Zachariassen, 2005). In order to eliminate operational complexity and low throughput problems associated with this method, a simple and fast screening method for analyzing AFPs is required.

Over the past two decades, colorimetric assays using gold nanoparticles (AuNPs) have received particular attention in the field of clinical and environmental diagnosis, due to their simplicity and low cost. Typically, a change in the color of the AuNP solution is caused by particle aggregation (or agglomeration) and light scattering-assisted surface plasmon (Anker et al., 2008; Elghanian et al., 1997; Rosi and Mirkin, 2005; Stewart et al., 2008; Xia et al., 2010), which is visible with the naked eye and is simply quantified through the extinction spectrum. Although such methods are well established in many bioassays, most of them are based on the interaction between target molecules and surface ligands on the AuNP; on the other hand, there has been very little research on the frozen assemblies of AuNPs for biochemical assays. Since AuNPs (or Au nanorods) are known to be easily aggregated at subzero temperatures due to surface disruption by ice crystals (Albert et al., 2009; Lewis et al., 1997; Zhang et al., 2008), it would be possible to screen cryoprotectants using this principle. However, controlling the frozen assembly of AuNPs still remains a challenge because it may be caused not only by ice crystallization but also by many other factors such as the

* Corresponding author at: Department of Life Science, Hanyang University, Seoul 133-791, Republic of Korea. Tel.: +82 2 2220 2561; fax: +82 2 2299 2561.

** Corresponding author at: Department of Life Science, Hanyang University, Seoul 133-791, Republic of Korea. Tel.: +82 2 2220 2560; fax: +82 2 6280 6725.

E-mail addresses: esjin@hanyang.ac.kr (E. Jin), ypilkim@hanyang.ac.kr (Y.-P. Kim).

surface functionality of the AuNPs and the freezing conditions. Nonetheless, to broaden the scope of nanosensors, it is valuable to investigate the interactions at subzero temperatures between nanoparticles and proteins while the diverse AFPs act as inhibitors of ice growth. Although the freezing properties of AuNPs with proteins need to be explored, to our best knowledge, there has been no attempt to analyze the activity and stability of proteins using a frozen assembly of AuNPs.

Herein we report the rapid analysis of AFP activity based on the self-assembly of AuNPs at subzero temperatures. We chose two different AFPs for our assay: *CnAFP* from the Antarctic diatom *Chaetoceros neogracile* and *LeIBP* from the Arctic yeast *Leucosporidium* sp.. The genes coding these AFP were recently cloned and their activities at the protein level have been studied (Gwak et al., 2010; Lee et al., 2010, 2012). Compared to the more well-known AFPs from cold-adaptive fish (Marshall et al., 2004; Siccheri and Yang, 1995; Tachibana et al., 2004), *CnAFP*s and *LeIBP*s can be expressed in *Escherichia coli* for the purpose of mass production. Furthermore, it should be noted that their non-glycosylated forms have been shown to retain antifreeze activity and recrystallization inhibitory effects (Gwak et al., 2010; Lee et al., 2010, 2012), which, in turn, were used in the present study as excellent model proteins so as to compare their activities and stabilities. The assembly and disassembly of AuNPs were also investigated in terms of concentrations and loss-of-function mutations of two AFPs and the resulting data were compared to the TH values of two AFPs.

2. Materials and methods

2.1. Chemicals

Hydrogen tetrachloroaurate(III)trihydrate ($\text{HAuCl}_4 \cdot 3\text{H}_2\text{O}$, 99.9%), sodium citrate dihydrate (trisodium salt, $\text{C}_6\text{H}_5\text{Na}_3\text{O}_7 \cdot 2\text{H}_2\text{O}$), mercaptosuccinic acid (MSA, $\geq 99.0\%$), and bovine serum albumin (BSA, $\geq 96\%$) were purchased from Sigma–Aldrich. Carboxymethylpoly(ethylene) glycol-thiol (CM-PEG-SH, MW 1000) was purchased from Laysan Bio Inc. (U.S.A.). All the chemicals were of analytical grade and were used as received.

2.2. Synthesis of AuNPs

To generate MSA-capped AuNPs, citrate-stabilized AuNP (Cit-AuNP) was synthesized, as previously described (Grabar et al., 1995). Briefly, a stock solution (20 mL) containing 1 mM $\text{HAuCl}_4 \cdot 3\text{H}_2\text{O}$ was added to distilled water (50 mL) to give a final concentration of 300 nM in a round-bottom flask; this was brought to boiling temperature under vigorous stirring. Rapid addition of 2 mL of 30 mM sodium citrate to the stirring solution resulted in a color change from pale yellow to red brown. The solution was kept boiling for a further 20 min and was then cooled to room temperature while stirring. A further modification was performed by adding 2 mL of 30 mM MSA to the Cit-AuNP solution, followed by vigorous stirring at RT for 1 h. The molar ratio of tetrachloroaurate, sodium citrate, and MSA was 1:200:200. The average size of MSA-capped AuNPs was determined to be 15.8 ± 1.3 nm using a field emission scanning electron microscope (FE-SEM S-4800, Hitachi, Japan). In the case of carboxyl PEG-capped AuNP, 40 mg of CM-PEG-SH was added to the Cit-AuNP solution (20 mL of 12 nM), followed by vigorous stirring at RT. After a 2 h incubation, excess molecules were removed by repeated centrifugation ($22,000 \times g$ for 30 min, three times). The molar concentration of the MSA-AuNP solution was calculated by dividing the total number of gold atoms by the average number of gold atoms per NP, which was estimated diameter measurements and the reported equation (Cumberland

and Strouse, 2002). Based on the molar concentration, the extinction coefficient of MSA-AuNP was determined to be $1.7 \times 10^8 \text{ M}^{-1} \text{ cm}^{-1}$ at 520 nm by using UV–visible spectrophotometer (Cary 60 UV–vis, Agilent Technologies).

2.3. Expression of AFPs

The *CnAFP* protein was expressed in *E. coli* and purified through the unfolding–refolding process after inclusion body isolation. The gene encoding *CnAFP* was ligated into the *kpnI*/*HindIII* sites of the pCold I vector placing a N-terminal $6 \times \text{His}$ -tag on the protein. After being grown with isopropyl- β -D-galactopyranoside (IPTG) induction at 10–15 °C, the transformed *E. coli* cells were harvested by centrifugation, and the cell pellet was then washed with an equal volume of cell lysis buffer (20 mM Tris-Cl, pH 8.0, containing 0.5 M NaCl). Thereafter, the cell lysate were acquired after using a sonicator (Branson, U.S.A.), which was followed by the centrifugation at $20,000 \times g$ at 4 °C for 20 min. After decanting the supernatant, the remaining pellet was resuspended in pellet lysis buffer (50 mM Tris-Cl, pH 8.0, containing 1 mM EDTA and 100 mM NaCl) and subsequently treated with the inclusion-body solubilization buffer I (50 mM Tris-Cl, pH 8.0, containing 1 mM EDTA, 100 mM NaCl, 8 M urea, and 0.1 M PMSF) and buffer II (50 mM KH_2PO_4 , pH 10.7, containing 1 mM EDTA, and 50 mM NaCl) to unfold proteins in inclusion body. The soluble fraction was then harvested by high-speed centrifugation and the refolding process was undertaken by diluting the concentrated protein-denaturant solution into a refolding buffer (50 mM Tris-Cl, pH 8.0) using a dialysis membrane at 4 °C overnight, which allowed the formation of the native structure of the protein. The refolded *CnAFP* was purified by using Ni-NTA affinity chromatography (Qiagen, Germany). The final concentration of *CnAFP* was determined using the known extinction coefficient ($22,585 \text{ M}^{-1} \text{ cm}^{-1}$ at 280 nm) and UV–visible spectroscopy (Cary 60 UV–vis, Agilent Technologies). Wild type *LeIBP*, and mutants S147Y&A234Y, T65Y, S43Y, and A234Y were cloned into pET-28a vector (Novagen) and expressed in *E. coli* strain BL21-DE3 (Invitrogen) as described previously (Lee et al., 2012). Briefly, the transformed bacteria were grown at 37 °C in LB medium containing $20 \mu\text{g mL}^{-1}$ kanamycin. Bacterial cultures were induced when OD_{600} was 0.6 by adding IPTG (final 1 mM) and incubating at 30 °C for 24 h. Pelleted cells were resuspended in 50 mM NaH_2PO_4 , 300 mM NaCl and 5 mM imidazole. After lysis using sonication, the lysate was clarified by centrifugation (12,000 rpm for 1 h at 4 °C). The cell lysate was loaded on a Ni-NTA agarose column and washed extensively with 50 mM NaH_2PO_4 , 300 mM NaCl and 5 mM imidazole (25 column volumes). The bound protein was then eluted with a buffer consisting of 50 mM sodium phosphate (pH 8.5), 300 mM NaCl, 300 mM imidazole. After cleavage of the $6 \times \text{His}$ -tag at 4 °C overnight, the proteins were gel filtrated on a Superdex-200 column (Amersham) equilibrated in 20 mM Tris–HCl (pH 8.0) supplemented with 150 mM NaCl.

2.4. Measurement of thermal hysteresis (TH) and ice crystal morphology

The THs of purified recombinant *CnAFP* and *LeIBP* were assayed by a nanolitre osmometer (Otago Nanoliter-Mar Biotechnol osmometer, New Zealand) as described previously (Gwak et al., 2010; Lee et al., 2012). For this, the recombinant *CnAFP* and *LeIBP* were concentrated to 1 mg mL^{-1} and was then diluted with distilled water as appropriate. Solutions of BSA, known to have no AFP activity, were used as the negative controls. The TH assay was repeated three times. The sample cell was placed on the surface of a temperature-controlled metal block connected to nanoliter osmometer. The change in ice crystal morphology was also

monitored through the microscopic observation. The protein samples were loaded into the center of a freezing stage (Otago Nanoliter-osmometer, New Zealand) and observed the attached microscope (Olympus BX53). The freezing was carried out at $-20\text{ }^{\circ}\text{C}$ for 5 min, after which samples were thawed until one single crystal was present. Thereafter, temperature of the freezing stage was slowly lowered to a rate of $0.01\text{ }^{\circ}\text{C min}^{-1}$ to observe ice crystal growth. The ice crystal images were captured under microscope using a CCD camera (DMCe 310). In this assay, ice crystals that are a circular disk shape when grown in solution indicate the absence of antifreeze activity, while hexagonally shaped ice crystals indicate the presence of antifreeze activity.

2.5. Colorimetric assay of AFP activity

An appropriate volume of either *CnAFP* (1 or $10\text{ }\mu\text{M}$) or *LeIBP* (10 or $40\text{ }\mu\text{M}$) was added to each well containing the MSA-AuNP solution ($100\text{ }\mu\text{L}$ at 4 nM) in the microwell plate, followed by the addition of distilled water up to $200\text{ }\mu\text{L}$. As a negative control, BSA was also used at the same range of concentration. The reactant on the microwell plate was placed under a cycle of freezing at $-20\text{ }^{\circ}\text{C}$ for 60 min and thawing at $37\text{ }^{\circ}\text{C}$ for 10 min. Before and after the freezing/thawing cycle, the extinction spectrum was obtained by using a UV-vis spectrometer (Cary 60 UV-vis, Agilent Technologies) or absorbance microplate reader (Varioskan Flash, Thermo Fisher Scientific Inc.). For the stability test, two AFPs (*CnAFP* and *LeIBP*) was initially subjected to 5 or 10 cycles of freezing at $-80\text{ }^{\circ}\text{C}$ for 20 min and thawing at $37\text{ }^{\circ}\text{C}$ for 10 min, and the AFPs with and without repetitive freeze-thaw cycle were then added to the MSA-AuNP solution. Next, the AuNP-mixture on the microwell plate was placed again under a cycle of freezing at $-20\text{ }^{\circ}\text{C}$ for 60 min and thawing at $37\text{ }^{\circ}\text{C}$ for 10 min to generate the AuNP aggregation. To quantify this, the aggregation parameter (E_{520}/E_{650}) of the AuNP solution on the well was compared using the microplate reader.

3. Results and discussion

As depicted in Scheme 1, we reason that the ideal AFP should be capable of impeding frozen aggregation of AuNPs, due to its preferential binding to ice crystals, resulting in a strong scattering peak at near 520 nm in the extinction spectrum. On the other hand, AFP-free conditions cause AuNPs to be self-assembled during the freezing/thawing process, resulting in a color change from red to blue.

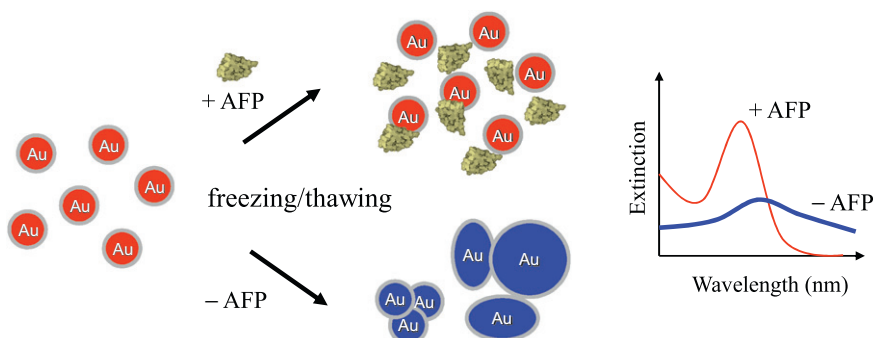
3.1. Effect of frozen assembly of AuNPs on AFP (or IBP) activity

To check this possibility, the *CnAFP* was purified from *E. coli* and reacted with the solution of AuNPs at a cycle of 1 h freezing at $-20\text{ }^{\circ}\text{C}$

and 10 min-thawing at $37\text{ }^{\circ}\text{C}$. To induce a large change in particle aggregation, 16 nm-AuNP modified with mercaptosuccinic acid (MSA) were used in the present study (Fig. S1). As a result of the freezing/thawing process, the MSA-capped AuNP (MSA-AuNP) with bovine serum albumin (BSA) was evenly aggregated over the given concentration range of BSA ($0.1\text{--}2\text{ }\mu\text{M}$) (Fig. 1A upper column). The protein-free AuNP solution (lane 1, Fig. 1A) was also completely aggregated and had changed to a blue color after the freezing/thawing cycle. By contrast, as the concentration of *CnAFP* increased the MSA-AuNP did not change color (i.e. no freeze-induced aggregation) (Fig. 1A bottom column). When the degree of aggregation was quantified by the extinction ratio (E_{520}/E_{650}) (Fig. 1B), there was a linear correlation between the extinction ratio and *CnAFP* concentration ($0.1\text{--}2\text{ }\mu\text{M}$) (Fig. 1C). AFP activity was also associated with a hexagonal ice crystal morphology, which was in contrast to that observed for BSA (Fig. 1D). Similar to *CnAFP*, *LeIBP* resulted in a concentration-dependent color change by protecting the freeze-induced assembly process of AuNPs, but the detection range of *LeIBP* was different to that of *CnAFP*; a relatively higher concentration ($1\text{--}20\text{ }\mu\text{M}$) of *LeIBP* was able to be quantified under the same conditions (Fig. 2A and B). Considering the similar molecular weights of the two AFPs (*CnAFP*, 29 kDa (Gwak et al., 2010); *LeIBP*, 25 kDa (Lee et al., 2012)), it is presumed that the antifreezing activity of *CnAFP* would be slightly higher than that of *LeIBP*. It is also noteworthy that the TH value of *CnAFP* (maximum $0.8\text{ }^{\circ}\text{C}$ at $33\text{ }\mu\text{M}$) (Gwak et al., 2010) was found to be higher than that of *LeIBP* (maximum $0.3\text{ }^{\circ}\text{C}$ at $300\text{ }\mu\text{M}$) (Lee et al., 2012), which was consistent with our results. In terms of AFP concentration, the detection sensitivity of our system was approximately 100-fold higher than those of TH measurement. Therefore, our result reveals that the AuNP-based colorimetric assay is well suited to the analysis of AFP activity, due to its high sensitivity and simplicity.

3.2. Analysis of AFP activity with different AuNPs

Intriguingly, among the tested AuNPs, MSA-AuNPs only gave rise to a significant difference in the frozen assembly between BSA and AFP. Citrate-stabilized AuNPs (Cit-AuNP), which are generally used in colorimetric assays, did not differentiate the frozen assembly between BSA and AFP, wherein BSA made Cit-AuNPs stable by surface binding via cysteine residues at its outmost, endowing the improved resistance to self-assembly of AuNPs at freezing temperature (Fig. S2). The AuNPs modified by thiol-terminated polyethylene glycol (PEG) were highly stable and, consequently, they were rarely aggregated even after the freezing/thawing cycle (Fig. S3). Moreover, the MSA-AuNP was made by the addition of a low-dose of MSA (equivalent to the citrate concentration) to the solution of Cit-AuNPs, which was only effective to detect AFP activity; neither AuNPs made from



Scheme 1. Schematic of AuNP-based colorimetric assay of AFP activity. In the presence of AFP, the self-assembly (blue) of 16-nm-AuNP (red) is strongly inhibited after a freezing/thawing cycle, and the freeze-induced assembly can be quantified by the extinction spectrum. (For interpretation of the references to color in this figure caption, the reader is referred to the web version of this article.)

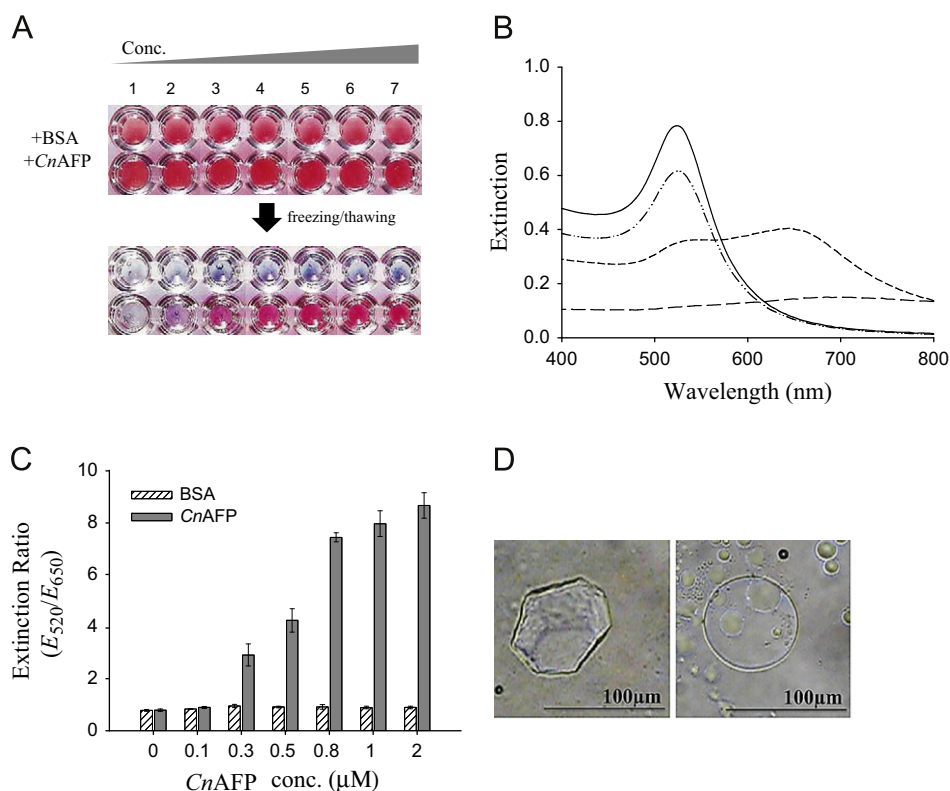


Fig. 1. AuNP-based colorimetric assay of CnAFP activity. (A) The MSA-AuNP solution (2 nM) mixed with either BSA (upper column) or CnAFP (bottom column) in the microwell plate was pictured before and after the freezing/thawing cycle (1 h at $-20\text{ }^{\circ}\text{C}$ and 10 min at $37\text{ }^{\circ}\text{C}$). The protein concentration range used is represented by the numbers 1–7, which correspond to 0, 0.1, 0.3, 0.5, 0.8, 1, and 2 μM , respectively. (B) Extinction spectra after freezing/thawing: MSA-AuNP (dotted line), MSA-AuNP + 2 μM BSA (dash line), and MSA-AuNP + 2 μM CnAFP (dash-dot line). The solid line is the extinction spectrum of control MSA-AuNP solution before freezing/thawing. (C) The AuNP aggregation as seen in (A) was quantified by the extinction ratio (E_{520}/E_{650}). The error bars represent the standard deviation from triplicate independent experiments. (D) Microscopic images of ice crystals formed in the presence of CnAFP (left) and BSA (right). (For interpretation of the references to color in this figure caption, the reader is referred to the web version of this article.)

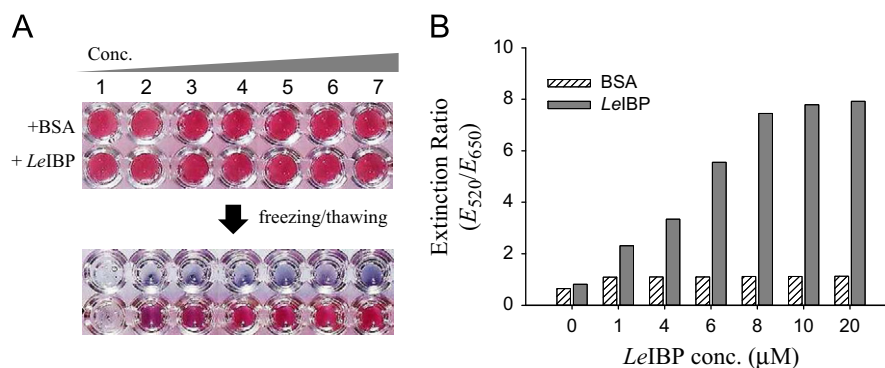


Fig. 2. AuNP-based colorimetric assay of LeIBP activity. (A) The MSA-AuNP solution (2 nM) mixed with either BSA (upper column) or LeIBP (bottom column) in the microwell plate was pictured before and after the freezing/thawing cycle (1 h at $-20\text{ }^{\circ}\text{C}$ and 10 min at $37\text{ }^{\circ}\text{C}$). The protein concentration range used is represented by the numbers 1–7, which correspond to 0, 1, 4, 6, 8, 10, and 20 μM , respectively. (B) AuNP aggregation as seen in (A) was quantified by the extinction ratio (E_{520}/E_{650}).

MSA and gold seed ions nor the addition of a high-dose of MSA to Cit-AuNPs detected AFP activity (data not shown). Although a mechanism explaining the relationship between protein structure and ice-binding crystals on the surface of AuNPs still remains unclear, it is likely that MSA loosely bound to the AuNP might be involved in both stabilization of the AuNP surface and ice crystallization during the freezing process.

3.3. Analysis of AFP activity using ice-binding mutants

To examine whether AuNP assembly is specific to AFP activity, LeIBP mutants with different antifreezing activities were tested, and

non-functional LeIBP was created by mutating the ice-binding site. The activities of such mutants have been verified by TH measurement, which represented that S147Y&A234Y, T65Y, S43Y, and A234Y mutants have the reduced antifreeze activities (23, 28, 35, and 47%, respectively), compared to wild-type LeIBP (100%). Upon the addition of these LeIBPs, our detection system clearly showed an activity-dependent color change; more aggregation was observed with mutants with lower activity after the freezing/thawing cycle. The extinction ratios measured in these experiments were similar to those found in the TH assay (Fig. 3A and B). Based on this result, we suggest that the assembly and disassembly of AuNPs can be attributed to the activity of AFP during the freezing process.

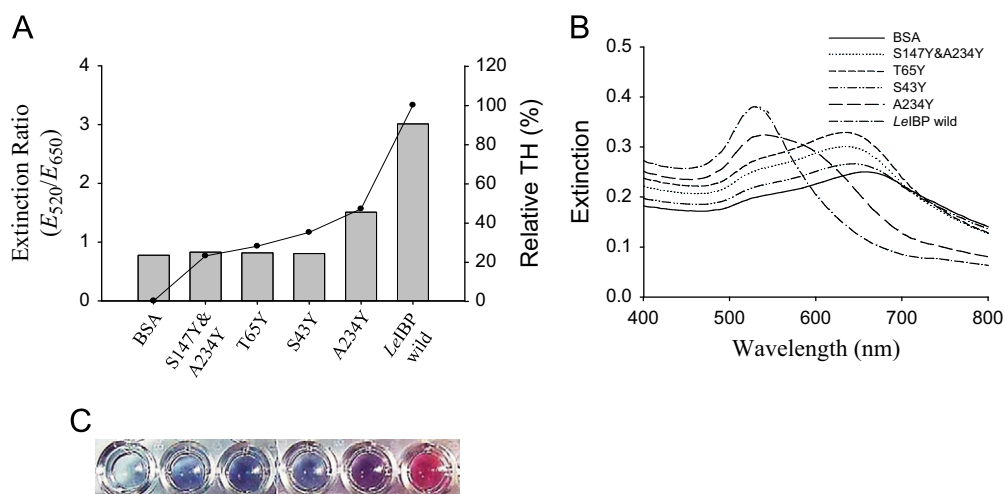


Fig. 3. Comparison of *LeIBP* mutants with different activities using the AuNP-based colorimetric assay. (A) The bar graph represents the extinction ratio of MSA-AuNPs mixed with BSA control and different *LeIBPs* (S147Y&A234Y, T65Y, S43Y, and A234Y mutants, and wild type) after the freezing/thawing cycle. The relative TH activity of the corresponding proteins is displayed as a solid line. The protein concentration used was 5 μ M. (B) Extinction spectra of MSA-AuNPs (2 nM) with different types of proteins after the freeze/thaw cycle. (C) The color change in the MSA-AuNP solution from (A) is given below each bar graph. (For interpretation of the references to color in this figure caption, the reader is referred to the web version of this article.)

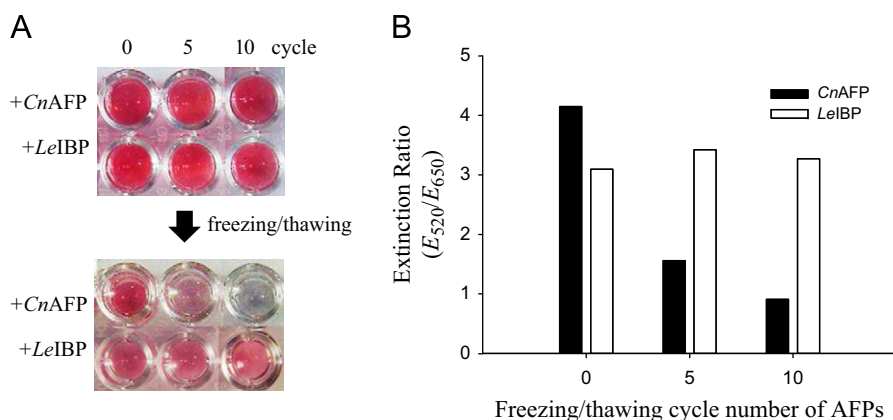


Fig. 4. (A) AuNP-based stability test on two AFPs after repetitive freezing/thawing cycles (5 and 10), and (B) changes in the extinction ratio of *CnAFP* (black bar) and *LeIBP* (white bar). (For interpretation of the references to color in this figure caption, the reader is referred to the web version of this article.)

3.4. Analysis of AFP stability

We next examined the stability of AFPs using the AuNPs. To accomplish this, the two AFPs (*CnAFP* and *LeIBP*) were subjected to harsh conditions (5 and 10 cycles of 20 min-freezing at -80°C and 10-min thawing at 37°C), and AFP was added to MSA-AuNPs at each cycle, followed by a further freezing/thawing treatment to induce the AuNP color change. Taking into consideration the detection range of the two proteins, we employed relatively low concentrations (200 nM for *CnAFP* and 1 μ M for *LeIBP*) from the standard curves shown in Figs. 1 and 2. In Fig. 4, the activity of *CnAFP* had markedly declined (i.e. color changed to blue) as the number of freezing/thawing cycle increased, whereas there was no color change in the solution containing *LeIBP*, regardless of the number of freezing/thawing cycles applied. In the case of *CnAFP*, at a relatively higher concentration ($> 1 \mu\text{M}$), the stability was less reduced under the repetitive freezing–thawing condition (data not shown). Although there is no direct evidence on the structural information of *CnAFP*, it is presumed that such instability of *CnAFP* might be due to the conformational change in the ice-binding domain by the temperature shock. Unlike *CnAFP*, *LeIBP* is reported to have high thermal stability even at a moderate or high temperature (Lee et al., 2012). This result clearly represents that the stability of *CnAFP* and *LeIBP* can be easily measured over repetitive freezing/

thawing while using a AuNP-based assay. Since there have been no reports regarding the stability of these AFPs, our results offer valuable insights into AFP activity and stability.

In addition to the inherent simplicity and cost-effectiveness, our system has more advantages over the conventional TH-based method. The method presented in this paper enables AFP activity to be detected with an approximately 100-fold higher detection sensitivity and at least 4-fold faster detection time over TH. TH measurements generally require a protein concentration exceeding the micromolar range, which is equal to more than milligram range per mL and generally require 6–24 h per test, depending on the toolkit. Not only can this system be applied to multiple AFPs simultaneously but it can also be extended to real-time measurement of AFP activity when combined with automated freezing/thawing.

4. Conclusions

In conclusion, we demonstrate that the frozen assembly of AuNPs was effectively harnessed to detect AFP activity. Owing to the ability of AFP to bind to ice crystals during freezing, MSA-AuNPs mixed with AFPs was not aggregated after the freezing/thawing process, unlike those mixed with activity-reduced AFP mutants or activity-free BSA. By employing this colorimetric method, the concentration-dependent

activity and stability of two AFPs (*CnAFP* and *LeIBP*) were quantitatively analyzed in a more facile way, and the results were significantly correlated with those of TH. Therefore, we anticipate that our method will find applications to study the physiological functions of many other AFPs from organisms native to cold climates in a high-throughput way.

Acknowledgment

This research was supported by the 2011 Polar Academic Program (PAP, PD11010) from KOPRI, and Basic Science Research Program (2012-0008222), the Bio-Signal Analysis Technology Innovation Program (2012-0006053) and Nano·Material Technology Development Program (2012035286) through the National Research Foundation of Korea (NRF) funded by the Ministry of Education, Science and Technology (MEST). This work was also supported by the Korea CCS R&D Center (KCRC) grant funded by the Korea government (MEST) (2011-0031999).

Appendix A. Supporting information

Supplementary data associated with this article can be found in the online version at <http://dx.doi.org/10.1016/j.bios.2012.09.052>.

References

- Albert, G.C., Roumeliotis, M., Carson, J.J.L., 2009. *Nanotechnology*, 20.
- Anker, J.N., Hall, W.P., Lyandres, O., Shah, N.C., Zhao, J., Van Duyne, R.P., 2008. *Nature Materials* 7, 442–453.
- Barrett, J., 2001. *International Journal of Biochemistry & Cell Biology* 33, 105–117.
- Boonsupthip, W., Lee, T.C., 2003. *Journal of Food Science* 68, 1804–1809.
- Carpenter, J.F., Hansen, T.N., 1992. *Proceedings of the National Academy of Sciences of the United States of America* 89, 8953–8957.
- Chou, K.C., 1992. *Journal of Molecular Biology* 223, 509–517.
- Cumberland, S.L., Strouse, G.F., 2002. *Langmuir* 18, 269–276.
- Elghanian, R., Storhoff, J.J., Mucic, R.C., Letsinger, R.L., Mirkin, C.A., 1997. *Science* 277, 1078–1081.
- Fletcher, G.L., Hew, C.L., Davies, P.L., 2001. *Annual Review of Physiology* 63, 359–390.
- Garnham, C.P., Campbell, R.L., Davies, P.L., 2011. *Proceedings of the National Academy of Sciences of the United States of America* 108, 7363–7367.
- Grabar, K.C., Freeman, R.G., Hommer, M.B., Natan, M.J., 1995. *Analytical Chemistry* 67, 735–743.
- Griffith, M., Yaish, M.W.F., 2004. *Trends in Plant Science* 9, 399–405.
- Gwak, I.G., Jung, W.S., Kim, H.J., Kang, S.H., Jin, E., 2010. *Marine Biotechnology* 12, 630–639.
- Jorov, A., Zhorov, B.S., Yang, D.S.C., 2004. *Protein Science* 13, 1524–1537.
- Kristiansen, E., Zachariassen, K.E., 2005. *Cryobiology* 51, 262–280.
- Lee, J.H., Park, A.K., Do, H., Park, K.S., Moh, S.H., Chi, Y.M., Kim, H.J., 2012. *Journal of Biological Chemistry* 287, 11460–11468.
- Lee, J.K., Park, K.S., Park, S., Park, H., Song, Y.H., Kang, S.H., Kim, H.J., 2010. *Cryobiology* 60, 222–228.
- Lewis, L.J., Jensen, P., Barrat, J.L., 1997. *Physical Review B* 56, 2248–2257.
- Marshall, C.B., Fletcher, G.L., Davies, P.L., 2004. *Nature* 429, 153–153.
- Rosi, N.L., Mirkin, C.A., 2005. *Chemical Reviews* 105, 1547–1562.
- Sicheri, F., Yang, D.S.C., 1995. *Nature* 375, 427–431.
- Stewart, M.E., Anderton, C.R., Thompson, L.B., Maria, J., Gray, S.K., Rogers, J.A., Nuzzo, R.G., 2008. *Chemical Reviews* 108, 494–521.
- Tachibana, Y., Fletcher, G.L., Fujitani, N., Tsuda, S., Monde, K., Nishimura, S.I., 2004. *Angewandte Chemie-International Edition* 43, 856–862.
- Xia, F., Zuo, X.L., Yang, R.Q., Xiao, Y., Kang, D., Vallee-Belisle, A., Gong, X., Yuen, J.D., Hsu, B.B.Y., Heeger, A.J., Plaxco, K.W., 2010. *Proceedings of the National Academy of Sciences of the United States of America* 107, 10837–10841.
- Zhang, L., Li, P., Li, D., Guo, S., Wang, E., 2008. *Langmuir* 24, 3407–3411.